Catalysis Today 212 (2013) 169–174

Contents lists available at SciVerse ScienceDirect

Catalysis Today

journal homepage: www.elsevier.com/locate/cattod

Effect of propylene glycol monomethyl ether and rust impurities on TS-1 deactivation in propylene epoxidation

Li Yi-chuan, Shen Ben-xian, Zhao Ji-gang*

State Key Laboratory of Chemical Engineering, East China University of Science and Technology, Shanghai 200237, China

ARTICLE INFO

Article history:
Received 14 March 2012
Received in revised form
14 September 2012
Accepted 18 September 2012
Available online 16 April 2013

Keywords:
Propylene oxide
TS-1
Catalytic performance
Deactivation
Characterization

ABSTRACT

The properties of TS-1 catalyst in continuous reaction of propylene epoxidation, as well as the effects of by-product propylene glycol monomethyl ether (PGME) on catalytic performance, was investigated in a low-pressure fixed bed reactor with chemical pure methanol as solvent. As the rust could be doped from the pipings and solvent containers, its impact on catalyst deactivation was then studied by using industrial-grade methanol. Finally the catalyst before and after deactivation was contrastively characterized by means of micro-structure analysis, TPD and TPR. The results showed that self-developed TS-1 catalyst performed well in the reaction, and the by-product propylene glycol monomethyl ether would not depress the catalytic activity in 80 h. The presence of rust could not only block active sites leading to partial loss of activity, but also increase the surface acidity, which would induce side reactions and decrease the selectivity of propylene oxide.

1. Introduction

As one of the important organic intermediate chemicals, more than four million tons of propylene oxide (PO) have been globally produced every year. However, in two traditional methods of manufacturing PO, chlorhydrin process has serious pollution to the environment whereas the co-oxidation process produces a large amount of joint products. Consequently, developing a short, clean process for producing PO is needed to replace the currently used industrial processes. Since the MFI-type titanosilicate, TS-1 was synthesized [1], direct epoxidation of propylene to propylene oxide (PO) over TS-1 using hydrogen peroxide (H_2O_2) as the oxidant, is regarded as the important development trend of PO green production [2–7], for its mild reaction conditions, high catalytic activity and high atom economy without pollution problems [2,3].

Although TS-1 gives excellent catalytic activity of the propylene epoxidation, the deactivation of the catalyst occurs on stream [8]. The deactivation mechanism of TS-1 is one of very important subjects in the industrialization of propylene epoxidation, but only a few reports on the TS-1 deactivation have been reported. Thiele et al. [3] thought that PO and the by-product propylene glycol monomethyl ether (PGME) could form oligomers within the zeolite micropores under acid catalysis reaction. With increasing chain length, the diffusivity of these oligomers decreases rapidly, until they literally get stuck in the zeolite pores and block the access of reactants to the catalytic sites. On the other hand, the activity of TS-1 for propylene epoxidation by hydrogen peroxide in methanol medium decreases due to titanium leaching from the catalyst framework [9]. Chen et al. [10] reported that pore plugging was resulted from by-products with large dimensions such as dimers or oligomers and leaching framework titanium would simultaneously deactivated the catalyst. On the basis of simulation experiment, Yan et al. [11] reported that the deactivation was mainly caused by the increasing amount of dimers and trimmers formed by PO. Liu et al. [12] studied deactivated catalyst by desorption in the presence of N_2, the deactivation mechanism they postulated was that adsorbed PO and PGME at active sites of TS-1 could suppress the catalytic activity, and the polyethers formed by PO and PGME, as well as the dimers and trimmers formed by PO could block the micropores or occupy the active sites.

In the present study, the performance of TS-1 catalyst in a continuous reaction system for propylene epoxidation, and the impact of the by-product PGME on catalytic activity are studied in a low-pressure fixed bed reactor with chemically pure methanol as solvent. Considering the corrosion of pipings and solvent containers in the pilot-plant, the influence of rust on TS-1 deactivation is exercised by using chemical-grade methanol as solvent under typically reaction conditions. Subsequently the mechanism of deactivation caused by rust is investigated by characterizing the sample of fresh and deactivated TS-1 catalyst.

---

* Corresponding author. Tel.: +86 2164252916.
E-mail addresses: zjg@ecust.edu.cn, zjg13122752231@hotmail.com (Z. Ji-gang).

0920-5861/$ – see front matter © 2013 Elsevier B.V. All rights reserved.
http://dx.doi.org/10.1016/j.cattod.2012.09.039

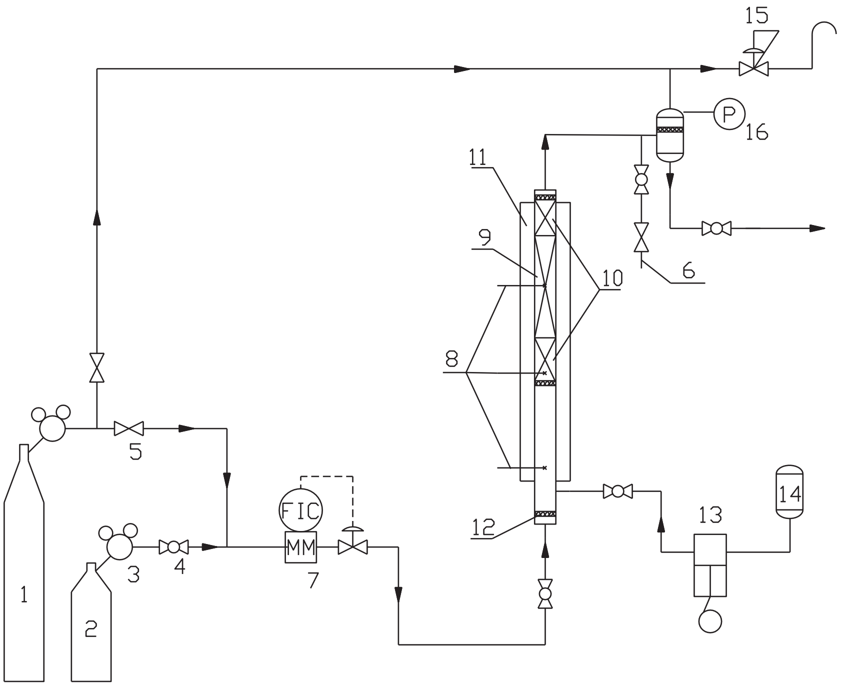

Fig. 1. Schematic diagram of experiment.

2. Experimental

2.1. Materials

Propylene (purity >95%) was provided by Gao Qiao SINOPEC (Shanghai, China). Hydrogen peroxide (30 wt%) was obtained from Jin Lu Co. Ltd (Shanghai, China). Methanol and propylene oxide were provided by Ling Feng Chemicals Co. Ltd (Shanghai, China). They were analytical reagent-grade.

2.2. Synthesis of TS-1

In a typical preparation [13], 1.92 g tetrapropylammonium bromide (TPABr, templating agent) was dissolved in 80 ml deionized water, then 20 ml colloidal silica NS-30(30 wt%, silica sources) was added under stirring for 1 h. Amounts of acetylacetone and tetrabutyl titanate (TBOT) were added in 10 ml isopropyl-alcohol orderly; this solution was called titanium alkoxide complex and was added and stirred for an hour, then 3.5 g *n*-butylamine was added. The mixture was then heated at 50 °C and 60 °C for an hour, respectively, under stirring.

The transparent gel, whose composition is as follows:

SiO_2:$x$$TiO_2$:0:06TPA:45$H_2O$where $0 < x < 0:04$ was then transferred into a Teflon-lined autoclave and was heated at 175 °C under autogenous pressure for three days.

After crystallization, the autoclave was cooled, and the solid was recovered by filtration. The zeolite was washed several times with deionized water and dried overnight at 110 °C in an oven. Occluded organics were removed by heating the sample in an air flow at 550 °C for about 6 h.

TS-1 molecular sieve catalyst was granulated according to the patent [14],the particle size of the catalyst used was from 20 mesh to 40 mesh.

2.3. Catalytic experiments

The experimental procedures of the direct epoxidation reaction are shown in Fig. 1. The epoxidation of propylene was carried out in a continuous-flow fixed bed reactor and its typical conditions [15] were listed in Table 1. The amount of catalyst loaded in the reactor was 4 g.

The residual H_2O_2 was measured by iodometric titration [16]. Reaction products were quantifiably calculated by a relative correction factor method [17] and analyzed on a HP-1 gas chromatography using a flame ionization detector and a capillary column (50 m × 0.32 m × 1.05 m). PO was the main product in this reaction, propylene glycol monomethyl ether (PGME) and propylene glycol (PG) were the byproducts. The reaction results were described by the following evaluating indicators:

$$\mathrm{H_2O_2\ conversion:}\ X_{H_2O_2} = \frac{n^0_{H_2O_2} - n^i_{H_2O_2}}{n^0_{H_2O_2}} \times 100\%$$

$$\mathrm{PO\ selectivity:}\ S_{PO} = \frac{n_{PO}}{n_{PO} + n_{PGME} + n_{PG}} \times 100\%$$

$$\mathrm{PO\ yield\ coefficient:}\ Y_{PO} = \frac{n_{PO}}{n^{id}_{PO}} \times 100\%$$

$X_{H_2O_2}$, S_{PO}, and Y_{PO} denote the conversion of H_2O_2, the selectivity of PO and the yields of PO, respectively. The n_{PO}, n_{PGME}, and n_{PG} stand for the number of moles of PO, PGME, and PG, respectively. The $n^0_{H_2O_2}$ and $n^i_{H_2O_2}$ were the initial mole content and the final mole

Table 1
Conditions of catalytic experiments.

Conditions	Details
Solvent	Methanol
Temperature/K	323
Pressure/MPa	0.7
Initial H_2O_2 concentration/wt%	2.1
Mole ratio of H_2O_2 to C_3H_6	1:2.5
WHSV of propylene/h^{-1}	2.1
LHSV of H_2O_2 solution/h^{-1}	32.4
Particle size of catalyst/meth	20–40
Reactor	PFR
Reactor dimensions	L/D = 50

Table 2
Instrumental and operating conditions for ICP-AES measurements.

Parameter	Type or amount
R.F. power (kw)	1.15
Carrier gas (Ar) flow rate (L min^{-1})	0.6
Auxiliary gas (Ar) flow rate (L min^{-1})	1.0
Coolant gas (Ar) flow rate (L min^{-1})	14
Nebulizer flow (psi)	30
Pump rate (r min^{-1})	100
Observation height (mm)	15
Integration time (s) on-axis	20
off-axis	5
Wavelength (nm)	Fe 259.940

content of H_2O_2, respectively. The n_{PO}^{id} represent the mole content of PO that all the H_2O_2 fully react with C_3H_6 would produce.

2.4. Characterization of TS-1

The crystal structure was identified by X-ray diffraction (XRD) (Rigaku D/max- 2550VB/PC) analyses using Cu-Kα radiation. Spectra were collected from $2\theta = 5°$ to $50°$ in $0.02°$ steps. The crystal morphology was examined by a scanning electron microscopy (SEM) (JEOL Model JSM-6360 LV, Japan). Framework IR spectra were recorded on a Nicolet Magna-IR550, using KBr wafers.

Inductively coupled plasma atomic emission spectrometry(ICP-AES) was used for Fe determination by an IRIS Advantage ER/S inductively coupled plasma spectrometer (TJA, USA). The operation conditions and the wavelengths were summarized in Table 2. The sample of TS-1 was pre-dissolved by aqua regia.

The micro-structure of TS-1 was analyzed on a Micromeritics ASAP 2020 including single- and multipoint BET (Brunauer–Emmett–Teller) surface area, Langmuir surface area, pore volume and pore-length distributions in the mesopore ranges by the BJH (Barrett–Joyner– Halenda) algorithm, and the distributions of micropore volume and pore size by the methods of H–K (Horvath-Kawazoe) with Saito & Foley model for cylindrical pores as well.

H_2-temperature-programmed reduction (H_2-TPR) was performed on a Micromeritics AutoChem II 2920 chemical adsorption instrument. Using mixture gas H_2–Ar (9.92% H_2) as reduction gas. Typically, the sample (0.2 g) was first pretreated in a quartz reactor with a high-purity He gas flow at 120 °C for 1 h. After the sample was cooled to room temperature, the H_2–Ar mixture was introduced into the reactor at a rate of 5 cm^3 min, and the temperature was raised to 700 °C at a rate of 10 °C/min. The consumption of H_2 was monitored by a thermal conductivity detector (TCD).

NH_3-temperature-programmed desorption (NH_3-TPD) was also carried out with the Micromeritics AutoChem II 2920 chemical adsorption instrument. Typically, the sample (0.2 g) loaded in the quartz tube was first pretreated with a high-purity He gas flow at 250 °C for 1 h. The adsorption of NH_3 was performed in an NH_3–He (9.93% NH_3) mixture for 0.5 h, and then the remaining or weakly adsorbed NH_3 was purged by high-purity He. TPD was performed in the He flow by raising the temperature to 800 °C at a rate of 10 °C/min. The desorbed NH_3 was detected by the mass spectrometer.

3. 2 Results and discussion

3.1. Catalytic performances

In order to prevent the formation of by-products, pH value of the feed solution in the tests using chemically pure methanol as solvent was adjusted to about 7 by ammonia solution (0.1 mol/L) [16]. The level of catalytic reaction is shown in Fig. 2, it is clearly that the TS-1 catalyst effectively catalyzes the epoxidation of propylene as both the H_2O_2 conversion and PO selectivity are maintained at about 90% during 140 h on steam, and therefore the stability is impressively good.

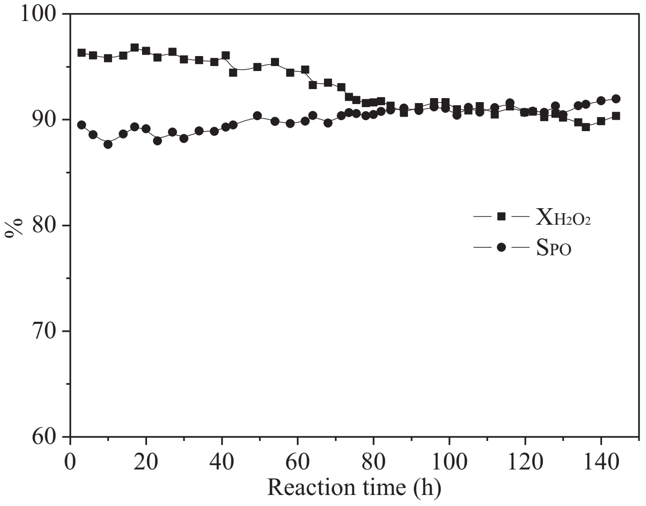

Fig. 2. Long-run test of the catalyst for propylene epoxidation.

3.2. PGME effect on catalytic performances

PGME is the overriding by-product of propylene epoxidation [16], formed by consecutive reactions of target reaction. Propylene epoxidation was operated in the reactor and PGME was added to the raw material (0.5 wt%) continuously. From the trend of $X_{H_2O_2}$, S_{PO}, and Y_{PO} shown in Fig. 3, it can be seen that the PO selectivity, H_2O_2 conversion and yield of PO are monotonous at about 85%, 68% and 57% in several, and they are distinctly stable along the reaction time with PGME injection.

Since the by-product formation is due largely to strong acid sites [3], the pH value of feed solution is adjusted to 5.5 for forcing the rate of PO selectivity to be reduced at about 80%, in order to further investigate the effect on catalyst of PGME. The reaction status is exhibited in Fig. 4, it is observed that during the reaction of approximately 80 h, the H_2O_2 conversion persists at 95% stably as before and the PO selectivity fluctuates slightly near 80% all the

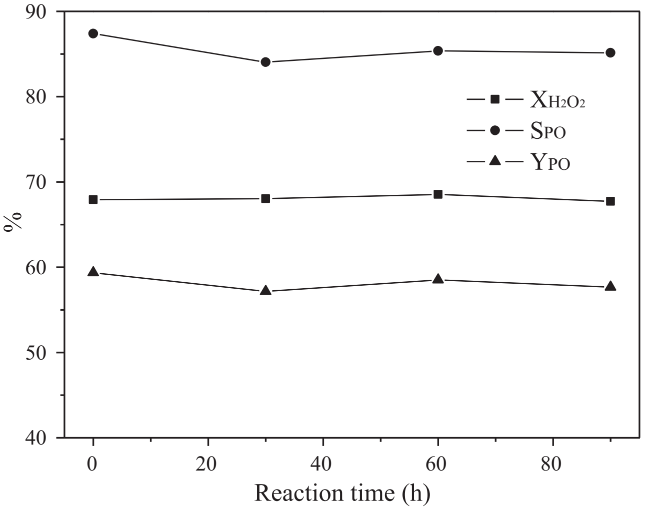

Fig. 3. Effect of PGME on catalytic performance for propylene epoxidation.

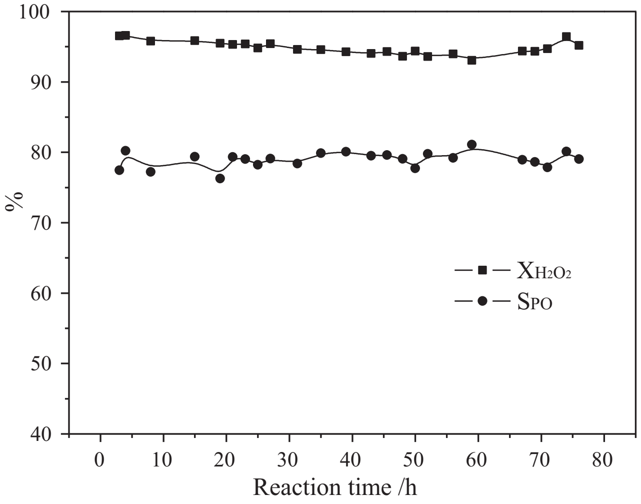

Fig. 4. Effect of by-product on catalytic performance for propylene epoxidation.

time, revealing that by-product PGME would not cause perceptible deactivation in this reaction system in at least 80 h.

3.3. Catalytic performances with rust impurities

At the time using industrial-grade methanol as solvent in the plant, the pipings of device and containers holding solvent could introduce rust impurities into reactor by the feed stream scouring. Feed solvent was pumped into reactor through a rusty pipe then epoxidation reaction was carried out under the typical conditions, and the catalytic performances were presented in Fig. 5. Only 60 h, H_2O_2 conversion, PO selectivity and the yield of PO started to fall and separately dropped by 12.5%, 20.4% and 25.8% until the reaction of 96 h, which illustrated that the rust do give rise to a certain loss in catalyst activity.

3.4. Characterization of TS-1 catalysts

The fresh TS-1 catalyst was named TS-1-FRESH. After the epoxidation of propylene with rust, the deactivated catalyst taken out of reactor was named TS-1-USED. Their X-ray diffraction patterns were shown in Fig. 6. The characteristic peaks attributed to the MFI structure obviously appeared in the patterns, while no peak was observed at $2\theta = 25.3°$ and a twin peak at $2\theta = 45°$. It was indicated that titanium was incorporated into the framework of TS-1 catalyst, and there was no distinct transformation occurred in crystal structure during the reaction with rust. This result can also be confirmed by their SEM images (Fig. 7).

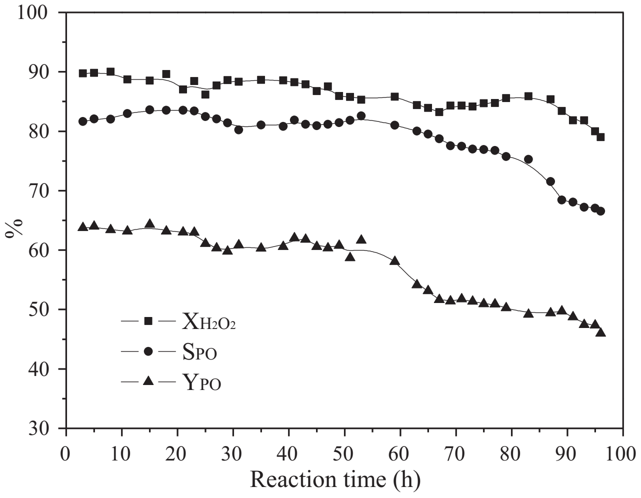

Fig. 5. Effect of rust in liquid feed on catalytic epoxidation of propylene.

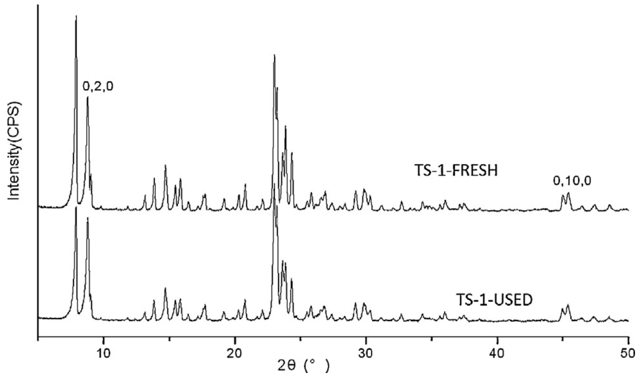

Fig. 6. XRD spectra of TS-1.

The image of TS-1-USED in Fig. 8a was absolutely different from the image of TS-1-FRESH in Fig. 8b. After reaction, the surface of catalyst was covered by a layer of tawny material. The measured concentration of Fe in TS-1-USED by ICP-AES was $9.058 \pm 0.010\ \mu g/g$. That means the tawny material was fine particles of rust. The infrared spectra in Fig. 9 exhibited a strong absorption band at $960\ cm^{-1}$ that revealed the existence of framework metallic ions and particularly framework Ti in TS-1. But the intensity of band at $960\ cm^{-1}$ of TS-1-USED was weakened as compared with TS-1-FRESH, this might be the result of combined effects of framework Ti and the rust adhered on catalyst.

The micro-structure analysis results are given in Table 3. As can be seen from the table, surface area and pore volume of catalyst all diminish for a certain extent after reaction, indicating that part of pores are covered by the rust so that the reactants cannot reach the active site resulting in the reduction of H_2O_2 conversion.

The micropore distribution by HK method and mesopore distribution by BJH method are depicted in Figs. 10 and 11. It can be observed that a loss of accessible micropore volume in the sorption isotherms occurred (Fig. 10), and the uniform distribution of mesopores disappeared (Fig. 11). After reaction the surface area, pore volume and distribution of TS-1 are probably altered by the blockage of channels resulting from the rust adsorbed.

Redox property of a catalyst is an important factor affecting its catalytic performances, particularly in selective oxidation reactions. The H_2 absorption peak appeared in the H_2-TPR process should be H_2 consumption peak during the sample was deoxidated by H_2, referred to as the H_2-TPR peak. The H_2-TPR profiles for the sample of TS-1-FRESH and TS-1-USED are shown in Fig. 12. A H_2-TPR peak is observed at 201.5 °C for the TS-1-USED sample while no obvious peak for the TS-1-FRESH sample, revealed that the TS-1 can be reduced after the catalyst is polluted by rust in feed solution. This result clearly indicates that the components from rust

Table 3
Micropore parameters of TS-1 catalyst before and after reaction.

Catalyst	Surface area/$m^2\ g^{-1}$			Pore volume/$cm^3\ g^{-1}$		
	S_{BET}	$S_{LANGMUIR}$	S_{sp}	S_{BJH}	V_{sp}	V_{BJH}
TS-1-FRESH	382	513	382	284	0.2197	0.1523
TS-1-USED	296	399	294	174	0.1816	0.1160

S_{BET}, multipoint BET surface area; $S_{LANGMUIR}$, Langmuir surface area; S_{sp}, single-point BET surface area ($P/P_0 = 0.20$); S_{BJH}, surface area of mesopores between 1 nm and 110 nm by the BJH method; V_{sp}, pore volume by single-point BET method ($P/P_0 = 0.983$, pore width less than 117 nm); V_{BJH}, cumulative desorption volume of mesopores between 1 nm and 110 nm by the BJH method.

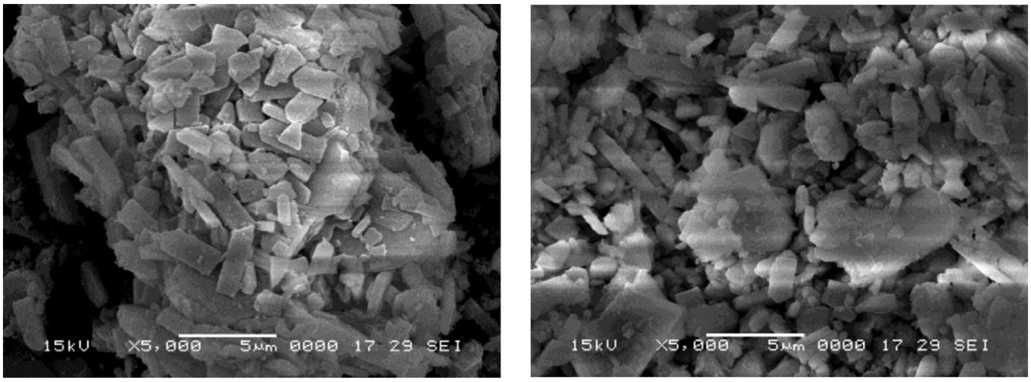

a TS-1-USED **b TS-1-FRESH**

Fig. 7. SEM image of TS-1.

a TS-1-USED **b TS-1-FRESH**

Fig. 8. Image of TS-1.

will be adsorbed on the TS-1 surface and the H_2-TPR peak is just the reduction peak for iron species. This further interpreted that the rust will cause deactivation of TS-1 zeolite catalyst in the propylene epoxidation.

As the acid sites are detrimental to propylene epoxidation over the TS-1 catalyst, the increase of surface acidity is likely to cause side reactions, reducing the selectivity of PO. NH_3-TPD curves of TS-1-FRESH and TS-1-USED are shown in Fig. 13. It is observed that the sample of TS-1-FRESH has one desorption peak at about 90 °C whereas the sample of TS-1-USED has another peak at higher temperature corresponding to relatively strong acidity. That means the amount of acidity on the catalyst surface is highly enhanced due to the appearance of the large number of stronger acid sites. It has been clarified that the joined rust can depress the catalytic performances by changing the number of acid sites on the TS-1 surface. This also confirms the situation that reducing the pH value of feed can promote the generation of PGME during the study in Section 2.2.

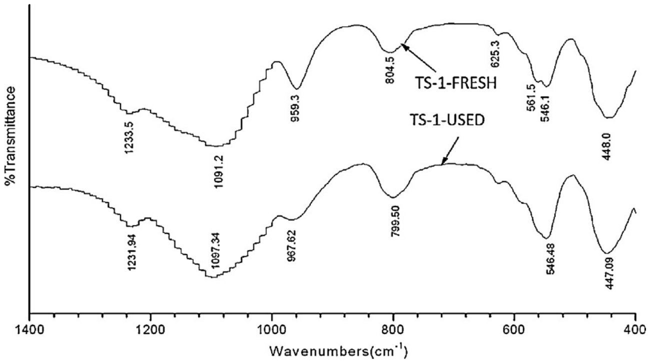

Fig. 9. IR spectra of TS-1.

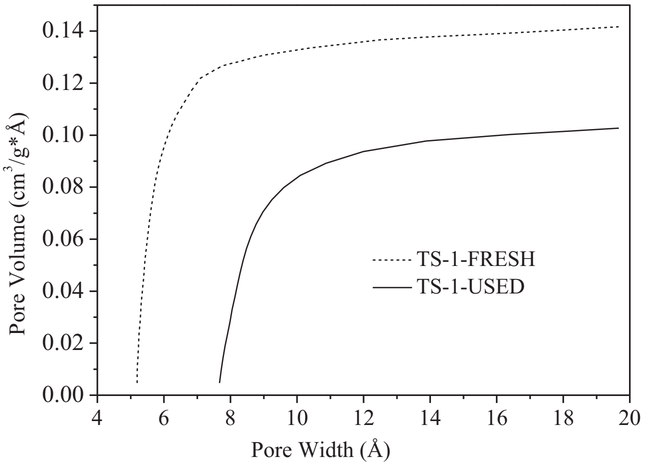

Fig. 10. H–K pore volume plot.

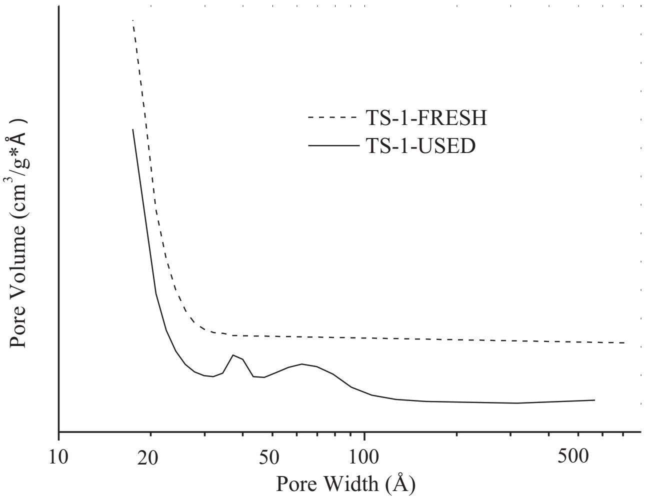

Fig. 11. BJH pore volume plot.

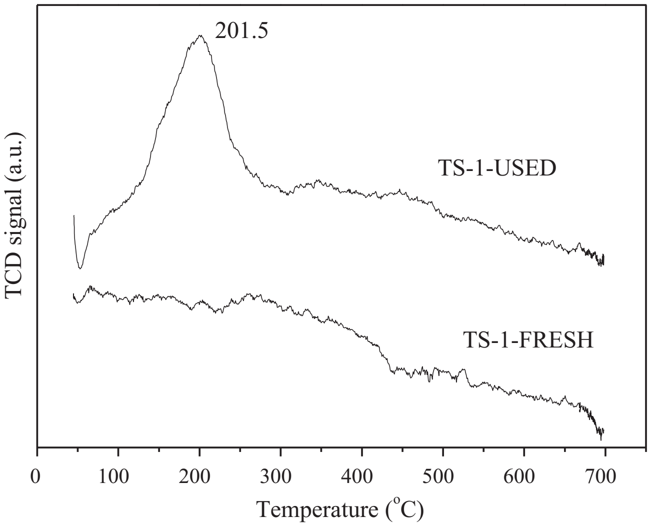

Fig. 12. H_2-TPR profiles of catalyst.

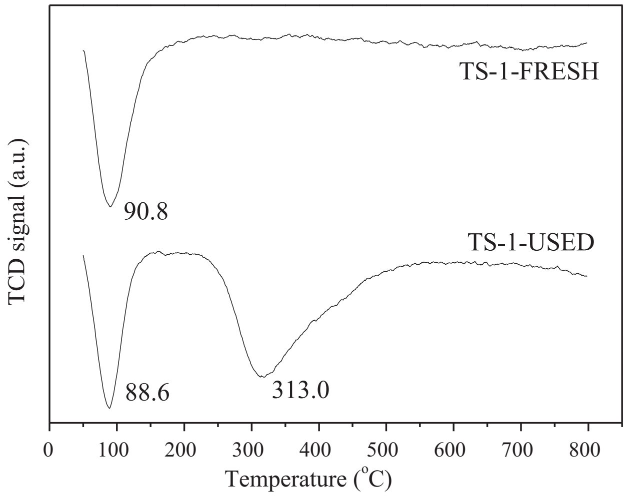

Fig. 13. NH_3-TPD profiles of catalyst.

4. Conclusions

The PO selectivity and H_2O_2 conversion of 90% were obtained during the reaction of approximately 140 h, while the by-product propylene glycol monomethyl ether would not disturb the catalytic activity over 80 h. Nevertheless, in the pilot-plant of PO, the components of rust from pipings and containers lead to a noticeable decline in the catalytic performance of propylene epoxidation, connected to not only decrease of BET surface area and surface morphology alterations but also significant increase of surface acidity. In order to raise the property and stability of TS-1 catalyst in epoxidation of propylene, the rust must be removed from the feedstock and the acidity of catalyst must be controlled in the pilot-scale test reaction systems.

Acknowledgements

We are grateful to the National High Technology Research and Development Program of China (863 Program: 2012AA040306) and Tianjin Dagu Chemical Co., Ltd. (China) for financial support.

References

[1] M. Taramasso, G. Perego, B. Notari, US Patent 4410 501 (1983).
[2] M.G. Clerici, G. Bellussi, U. Romano, Journal of Catalysis 129 (1991) 159–167.
[3] G.F. Thiele, E. Roland, Journal of Molecular Catalysis 117 (1997) 351–356.
[4] A. Tuel, Zeolites 16 (1996) 108–117.
[5] X.S. Wang, X.W. Guo, G. Li, Catalysis Today 74 (2002) 65–75.
[6] W. Liz, Urethane Technology 21 (2004) 4.
[7] C. Perego, A. Carati, P. Ingallina, M.A. Mantegazza, G. Bellussi, Applied Catalysis A: General 221 (2001) 63–72.
[8] Q.F. Wang, W. Li, J.X. Chen, Y.L. Wu, Z.T. Mi, Journal of Molecular Catalysis A: Chemical 273 (2007) 73–80.
[9] L. Davies, P. McMorn, D. Bethell, P. Page, F. King, F.E. Hancock, G.J. Hutchings, Chemical Communications 18 (2000) 1807–1808.
[10] J.X. Chen, Z.T. Mi, Y.L. WU, W. Li, Z.H. Li, Journal of Fuel Chemistry and Technology 31 (2003) 80–85.
[11] H.S. Yan, X.S. Wang, J. Liu, X.W. Guo, Acta Petrolei Sinica (Petroleum Processing Section) 18 (2002) 46–51.
[12] X.W. Liu, X.S. Wang, R.P. Wang, X.W. Guo, G. Li, Journal of Molecular Catalysis 17 (2003) 247–254(China).
[13] W.G. Xiao, B.X. Shen, J.G. Zhao, Y.T. Wei, C. Zhang, L. Wang, H. Ling, X. Chen, CN Patent 1751996 (2005).
[14] B.X. Shen, W.G. Xiao, J.G. Zhao, Y.T. Wei, Z.M. Zhang, H. Chen, L. Wang, C. Zhang, CN Patent 1911516 (2007).
[15] J.G. Zhao, B.X. Shen, W.G. Xiao, C. Zhang, L. Wang, Energy sources. Part A: Recovery, Utilization, and Environmental Effects 31 (2009) 108–117.
[16] J.G. Zhao, B.X. Shen, W.G. Xiao, C. Zhang, L. Wang, Acta Petrolei Sinica (Petroleum Processing Section) 21 (2005) 44–49.
[17] J.R. Jiao, B.X. Shen, J.G. Zhao, Energy Sources part A: Recovery, Utilization, and Environmental Effects 33 (2011) 1147–1154.